Observations of relativistic electron microbursts in association with VLF chorus

K. R. Lorentzen and J. B. Blake

Space Science Applications Laboratory, The Aerospace Corporation, Los Angeles, California

U. S. Inan and J. Bortnik

Space, Telecommunications and Radioscience Laboratory, Stanford University, Stanford, California

Abstract.
The Solar, Anomalous and Magnetospheric Particle Explorer (SAMPEX) satellite frequently observes relativistic (>1 MeV) electron precipitation in the radiation belts at L shells of 4–6 with bursty temporal structure lasting <1 s. This phenomenon can occur at all local times but is most often seen between 0200 and 1000 magnetic local time. VLF chorus is also observed to occur preferentially at these same local times. Using electron observations from the SAMPEX satellite Heavy Ion Large Telescope and data from the Polar satellite plasma wave instrument, we show correlation between observations of relativistic electron microbursts and VLF chorus with frequencies <2 kHz. In addition, the duration of the individual rising frequency chorus elements is comparable to the duration of the relativistic electron microbursts. It has been speculated that relativistic electron microbursts are caused by wave-particle interactions, which strongly scatter electrons into the loss cone for a short period. Lower-energy electron microbursts in the range from tens to hundreds of keV have long been associated with chorus waves, since these lower-energy electrons can resonate at the equator with whistler-mode waves at chorus frequencies. Electrons of MeV energies do not satisfy the first-order cyclotron resonance condition with chorus wave frequencies at the equator. However, MeV electrons may interact with chorus through higher-order resonances or off-equatorial interactions.

1. Introduction

Although the behavior of relativistic electrons in the radiation belts has been studied for many years, the source and loss mechanisms and their association with geomagnetic activity are still not well understood. A significant loss process is precipitation into the atmosphere, one form of which is relativistic electron microbursts. This phenomenon has been observed only in the last decade by *Imhof et al.* [1992], *Nakamura et al.* [1995, 2000], and *Blake et al.* [1996]. Relativistic electron microbursts last <1 s and have energies >1 MeV. They tend to have smaller fluxes than the lower-energy (>30 keV) microbursts first defined by *Anderson and Milton* [1964]. Detectors with large geometric factors are therefore needed to provide the time resolution necessary to observe electron microbursts at relativistic energies.

Blake et al. [1996] make the distinction between two types of relativistic electron precipitation (REP) seen by the Solar, Anomalous and Magnetospheric Particle Explorer (SAMPEX) satellite, which they term "bands" and "microbursts." These two types of precipitation can be generally distinguished by their duration as observed by low-altitude polar-orbiting satellites. Bands last >1 s, and microbursts last <1 s, although the two regimes can overlap. Bands generally occur singly or in small numbers, while microbursts can occur in trains of numerous bursts. The focus of this paper is on relativistic electron microbursts, but both types are discussed here in order to clarify the differences between the mechanisms proposed to account for these phenomena.

The REP bands are similar to the "spikes" observed by *Brown and Stone* [1972] and *Imhof et al.* [1986, 1991], near the trapping boundary of the radiation belts. Bands are often observed for several seconds or longer. They appear to be a spatial phenomenon rather than a temporal one, since the bands frequently recur on multiple passes through the radiation belts as well as being observed in the conjugate region. Generally, bands can be characterized by two features, pitch angle isotropy and selective energy dependence, which result from electron scattering in the current sheet. This current sheet scattering occurs when electron gyroradii become comparable to the radius of curvature of the magnetic field and electrons lose their adiabaticity [*Sergeev et al.*, 1983]. Because the Earth's magnetic field is stretched in the tail region, bands are most likely to occur on the nightside.

Relativistic electron microbursts, on the other hand, are observed near the nightside trapping boundary as well as on the dayside and at lower L shells, where the loss of adiabatic motion cannot account for the precipitation [*Lyons et al.*, 1999]. The highly structured microburst REP observed by

the SAMPEX satellite has been interpreted to be temporal in nature. Microburst electron packets have been observed over several bounce periods, and microbursts frequently display an abrupt rise and slower decay, regardless of the direction of travel of the spacecraft.

Plate 1 shows the latitudinal and local time distribution of the relativistic electron microbursts observed by SAMPEX at different levels of magnetic activity. The data show a weak maximum near midnight at low K_p values, but the maximum moves toward dawn at higher K_p values. The microbursts are more likely to occur when magnetic activity is high, and then they appear preferentially at magnetic latitudes between 60° and 66°, corresponding to L values between 4 and 6. Invariant latitudes and L shells used here and throughout this paper were determined using an eccentric dipole model. The >1 MeV electron microbursts observed by SAMPEX are usually accompanied by lower-energy (>150 keV) bursts with larger fluxes, although the bursts in the two energy channels do not usually exhibit a one-to-one correspondence [Blake et al., 1996]. It has been suggested that these relativistic electron microbursts are the result of wave-particle interactions, but the particular wave mode involved has not been identified.

Plasma wave observations from spacecraft such as OGO 3 [Burtis and Helliwell, 1976] and Spacecraft Charging at High Altitudes (SCATHA) [Koons and Roeder, 1990] show that chorus is also most likely to be observed between 0300 and 1500 magnetic local time (MLT). The overlap of chorus and REP microburst maxima in the morning sector suggests the need for a detailed examination of chorus as the precipitating agent for at least some of the observed microburst REP events. Chorus has long been associated with lower-energy X-ray and electron microbursts through wave-particle interactions near the equator [Oliven and Gurnett, 1968; Parks, 1978; Rosenberg et al., 1981, 1990; Roeder et al., 1985; Torkar et al., 1987]. Other observations of higher-energy relativistic electron precipitation from balloon-borne X-ray detectors have also been associated with wave activity, although these observations did not display temporal structure with timescales as short as the typical microburst [Rosenberg et al., 1972; Parks et al., 1979; Matthews et al., 1988]. Using a Sun-synchronous satellite, Imhof et al. [1992] studied relativistic electron microbursts at 2230 and 1030 MLT and found no correlation with ground-based chorus observations. Instead, they attributed their observations to a loss of stable trapping at the outer edge of the radiation belts. This mechanism is the same as that used by Blake et al. [1996] to account for the precipitation bands lasting several seconds or more. Although this mechanism may well account for the nightside microbursts occurring in small numbers near the trapping boundary, it cannot account for the microburst precipitation observed by SAMPEX at lower L shells and on the dayside.

In this paper we study relativistic electron microbursts and VLF wave activity using combined data from both the SAMPEX and Polar satellites. Although no examples of one-to-one correspondence between relativistic electron microbursts and VLF chorus were found, we present evidence that relativistic electron microbursts and VLF chorus are correlated in occurrence, and we suggest that chorus can, in fact, account for microburst electron precipitation at energies >1 MeV.

2. Instrumentation

The SAMPEX satellite was launched on July 3, 1992, into an orbit of 520 × 670 km altitude and 82° inclination [Baker et al., 1993]. The orbit period is ~96 min. The Heavy Ion Large Telescope (HILT) is sensitive to electrons when passing through the radiation belts and has a geometric factor of 60 cm² sr and a view angle of 68° × 68° [Klecker et al., 1993]. During the second half of 1996 and all of 1997, electrons with energies >1 MeV were sampled every 20 ms, although no data from the >150 keV channel were available. At this time the SAMPEX satellite was also spinning at a rate of one revolution per minute, giving greater pitch angle coverage than that earlier in the flight.

The Polar satellite was launched on February 24, 1996, into an orbit of ~9 × 1.8 R_E and an inclination of 86° [Harten and Clark, 1995]. The orbit period is ~18 hours. The plasma wave instrument (PWI) on this satellite includes a swept frequency receiver (SFR) that provides continuous single-component measurements of the electric and magnetic field from 26 Hz to 810 kHz and a high-frequency waveform receiver (HFWR) that provides three-component electric and magnetic field measurements from 20 Hz to 25 kHz, for short periods during each orbit [Gurnett et al., 1995]. Data from PWI are available from launch until September 17, 1997. Relativistic electron data from the Polar High Sensitivity Telescope (HIST) [Blake et al., 1995] were also used. This instrument measures trapped electrons in the radiation belt but cannot resolve the loss cone in any detail.

3. Observations

We compared data from Polar and SAMPEX for periods when the orbits of the two satellites were in approximately the same plane of local time. Table 1 gives the dates and magnetic local times for these periods. Because the local time of SAMPEX repeats once every 3 months and the local time of Polar repeats once every 6 months, the satellites were in the same sector approximately once every 6 months. Four 30-day periods of overlapping orbits were identified while PWI was operational. During these periods the satellites were always in predawn/postnoon orbits, giving somewhat limited coverage in local time but emphasizing the region where relativistic electron microbursts are most likely to occur (see Plate 1).

A typical example of relativistic electron microbursts and associated VLF chorus observed by SAMPEX and Polar in the predawn sector is shown in Plate 2. Plates 2a and 2b show >1 MeV electron data from the SAMPEX HILT detector as it passes through the radiation belts. The 30-s modulation is a result of the spacecraft spin. At this time the spacecraft is spinning such that the angle between the instrument look direction and the magnetic field ranges from 30°

Table 1. Overlapping Local Time Periods

Date	Days	Local Times, MLT
March 11 to April 9, 1996	71–100	0130–1330
August 31 to September 30, 1996	244–273	0215–1415
February 19 to March 20, 1997	50–79	0230–1430
August 10 to September 8, 1997	222–251	0315–1515

to 150°. However, the large view angle of the instrument allows it to sample electrons with pitch angles between 0° and 180°. A number of relativistic electron microbursts are visible between 1033:56 and 1034:16 UT, while the spacecraft is between $L = 4.7$ and $L = 5.1$ and with the detector positioned to sample electrons traveling along the field lines. Other isolated bursts are visible as low as $L = 3.6$ and as high as $L = 5.7$. The count rate during the bursts is lower than the count rate of the trapped electrons seen when the instrument is pointed perpendicular to the field lines. Although this difference in count rate implies that the loss cone is not filled, these data cannot be used to establish anisotropy without ambiguity, since the spatial scale of the precipitation is unknown. If the spatial scale is comparable to the gyroradius (~100 m), SAMPEX would pass through this region in less than the 20-ms sample period. Plate 2b shows 8 s of the bursts in more detail. The average burst duration is ~200 ms.

Plate 2c shows data from the PWI SFR as Polar travels north following a perigee pass. The upper hybrid resonance, f_{uhr}, increases suddenly at 1045 UT ($L = 3.3$), indicating the location of the plasmapause. The white line marked f_c shows the electron cyclotron frequency at the spacecraft. Intense chorus can be seen in a narrow band below this line between 1010 and 1040 UT. The range of chorus extends from $L = 5.1$ to $L = 3.4$. Because the satellite orbits did not coincide in such a way as to provide observations of microbursts while both satellites were located on exactly the same field line, we show two sets of PWI HFWR 0.45-s snapshots in Plates 2d and 2e. The snapshots within each set are separated by 9 s. Plate 2d shows data from 1017 UT, $L \sim 4.9$, approximately the same L shell where the bursts were observed by SAMPEX. Below ~2 kHz, chorus risers are clearly visible with duration ~200 ms, the same duration as the bursts. Plate 2e shows data from 1034 UT, $L \sim 3.8$, the same time that the bursts were observed by SAMPEX. Here chorus risers with duration of ~200 ms are very clear between 4 and 8 kHz.

Another example from the predawn sector is shown in Plate 3. Here the spacecraft is spinning such that the angle between the instrument look direction and the magnetic field ranges from 25° to 155°. During this pass there are fewer trapped particles, because the spacecraft mirror point was on the east side of the South Atlantic Anomaly and the bounce loss cone was >80°. In Plate 3a the relativistic electron microbursts are observed during the entire pass, from $L = 3.9$ to $L = 5.3$. Here the magnitude of the bursts approaches that of the trapped electrons, implying an isotropic pitch angle distribution. Plate 3b shows 6 s of the most intense bursts, which again have a duration of ~200 ms. Plate 3c shows intense chorus between 0304 and 0314 UT, continuing at a lower intensity until at least 0334 UT. The range of chorus extends from $L = 3.2$ until at least $L = 5.5$. Plate 3d shows data from 0324 UT, at approximately the same L shell where the strongest bursts were seen by SAMPEX. Chorus risers with a duration ~200 ms are visible below 2 kHz. At 0333 UT, the same time that the bursts were seen SAMPEX, Plate 3e shows weak chorus risers below 1 kHz.

An example from the postnoon sector is shown in Plate 4. Here the spacecraft is spinning such that the angle between the instrument look direction and the magnetic field ranges from 30° to 150°. In Plate 4a the relativistic electron microbursts are less intense and are again observed when the instrument is positioned to sample electrons traveling along the field lines. Plate 4b shows that these bursts have a somewhat longer duration of ~500 ms. In Plate 4c, chorus extends from 0545 to 0630 UT ($L = 6.5$–4.7). No Polar HFWR data are available from L shells greater than 4.8, but Plate 4d shows an example of an isolated chorus riser coming out of a hiss band at $L = 4.5$. This riser lasts over 400 ms and is similar to others seen during this pass. Plate 4e shows data from the same time as the bursts were observed, but the chorus had died out by the time Polar reached this location.

Although SAMPEX observations of relativistic electron bursts did not always coincide with times when the HFWR was on, we studied in detail the events that were found during the second and third interval defined in Table 1. These two intervals were chosen because the instrument modes were favorable for this study. During these intervals, HFWR data were available coincident with 29 relativistic electron microburst events. Of these, 9 occurred on the duskside, and 20 occurred on the dawnside. Chorus was observed at the same L shells as the microbursts for 22 of the 29 events. No chorus was observed for seven of the events, all of which occurred just after midnight.

In order to expand this study to facilitate comparison with magnetospheric activity, we also examined the occurrence of relativistic electron microbursts and chorus from times when the two spacecraft were not close to the same field lines. Plate 5 shows data from August 31 to September 30, 1996 (days 244–273). Dst and K_p show that this period was somewhat active, although there were no major storms. Plates 5c and 5d show histograms of occurrence frequencies for relativistic electron microbursts and chorus. Relativis-

tic electron microburst events were selected automatically by comparing the average count rate in a 100-ms period to a 500-ms running average. If the difference exceeded 10 times the standard deviation of the running average, the pass was identified as containing microbursts. SAMPEX data are accumulated in ~18-hour bins centered around the time of each Polar perigee pass. Dawnside passes are those occurring with 0000<MLT<1200 and duskside passes are those with 1200<MLT<2400. Chorus occurrence was recorded in minutes as observed by Polar as it passed through the Northern Hemisphere during each ~18-hour orbit. Chorus was determined from the continuous SFR plots, with confirmation from the HFWR when available. Although the chorus and microburst occurrence show only moderate correlation, the discrepancies may be accounted for by differences in the orbits of the two satellites and by the fact that chorus was frequently observed in the absence of relativistic electron microbursts.

Plates 5e and 5f show data from the 2.2-MeV channel of the HIST instrument on Polar. Plate 5e shows where the electrons peaked in L shell along with the dawnside plasmapause location as determined from the PWI upper hybrid resonance. Because it was not possible to use the upper hybrid resonance to find the plasmapause for all passes, the location of the inner plasmapause boundary was also calculated from the formula $L_{\mathrm{ppi}} = 5.6 - 0.46 K_{pmax}$, where K_{pmax} is the maximum K_p value in the preceding 24 hours [*Carpenter and Anderson*, 1992]. The peak in trapped relativistic electrons shows a small change in position, from $L = 4.4$ to $L = 4.7$, following the decrease in Dst and the increase in K_p on day 254. At the same time, the plasmapause is observed to move inward.

Plate 5f shows the peak count rate of 2.2-MeV electrons observed by Polar in a given outer zone traverse on the high-altitude (Northern Hemisphere) and low-altitude (Southern Hemisphere) portions of its orbit. The separation between high- and low-altitude points gives a measure of the isotropy of the pitch angle distribution [see also *Blake et al.*, 2001. Around day 254 the relativistic electron flux becomes slightly more anisotropic as the overall count rate decreases and subsequently increases. The adiabatic "Dst effect" [*Li et al.*, 1997; *Kim and Chan*, 1997] accounts for some, but not all, of this decrease and increase in relativistic electrons. Therefore nonadiabatic effects such as electron precipitation may also be important, particularly during the time when the count rate is increasing and the microburst occurrence is peaking. Most noteworthy is the fact that the increase in the SAMPEX relativistic electron microbursts is coincident with both the increase in Polar electron flux and the motion of the plasmapause to well inside the location of the peak flux.

Plate 6 shows data from February 19 to March 20, 1997 (days 50-79). Dst shows that there was a moderate geomagnetic storm on day 59, and K_p shows a corresponding increase at this time. Following this storm, K_p was somewhat lower than that for the 1996 interval shown in Plate 5. The occurrence of relativistic electron microbursts shows a distinct increase during the recovery phase of the storm.

The chorus occurrence shows a slight but less pronounced increase at this time.

Plates 6e and 6f show 2.2-MeV electron data from Polar, along with the plasmapause location determined as described above. Here the peak in trapped relativistic electrons is observed to move from $L = 4.0$ to $L = 4.5$ during the storm. At the same time, the position of the plasmapause is observed to move inward, inside the peak in relativistic electron flux. In addition, the relativistic electrons become highly anisotropic during the recovery phase of the storm, as shown by the separation of the high- and low-altitude count rate. It is generally assumed that strong radial diffusion during storms transports a seed population, perhaps substorm generated, into the region L ~3.5–4.5, where the relativistic electron peak is seen. The relativistic electron microbursts are closely time correlated with the increase in the relativistic electrons observed by Polar, and we suspect that the bursty precipitation leads to the flat electron pitch angle distribution.

The PWI data were also used for several additional tasks. When visible, the upper hybrid resonance frequency was used to identify the location of the dawnside plasmapause, as shown in Plates 5e and 6e. Almost all of the predawn relativistic electron microbursts were found to occur well outside of the plasmapause location. The upper hybrid resonance frequency was also used to calculate the cold plasma density on the L shell where the bursts were observed. These densities were compared to values obtained from the spacecraft potential obtained by the electric field instrument (EFI) on Polar [*Laakso et al.*, 1997] and were found to be consistent for the three examples shows in Plates 2-4. In addition, the six-component HFWR data were used to calculate wave normal angles for selected risers using the method of *Lauben et al.* [1998]. Typical values were found to be ~30°. Information on density and wave normal angles is essential for the cyclotron resonance calculations described in section 4.

4. Analysis

The cyclotron resonance interaction can only occur if the following condition is satisfied:

$$\omega + k \cos\theta \, v \cos\alpha = s\Omega_e/\gamma. \tag{1}$$

Here ω is the wave frequency, k is the wave number, θ is the wave propagation angle with respect to the magnetic field, v is the electron velocity, α is the electron pitch angle, s is an integer, Ω_e is the unsigned electron gyrofrequency, and γ is the relativistic mass factor. Here we have used the convention that both k and v are positive, although waves and particles must travel in opposite directions for whistler-mode waves to resonate with electrons having small pitch angles. If this resonance condition is satisfied, waves and particles can exchange energy, causing pitch angle scattering and precipitation.

Whistler-mode waves are right-hand circularly polarized waves whose cold plasma dispersion relation for quasi-longitudinal propagation is given by
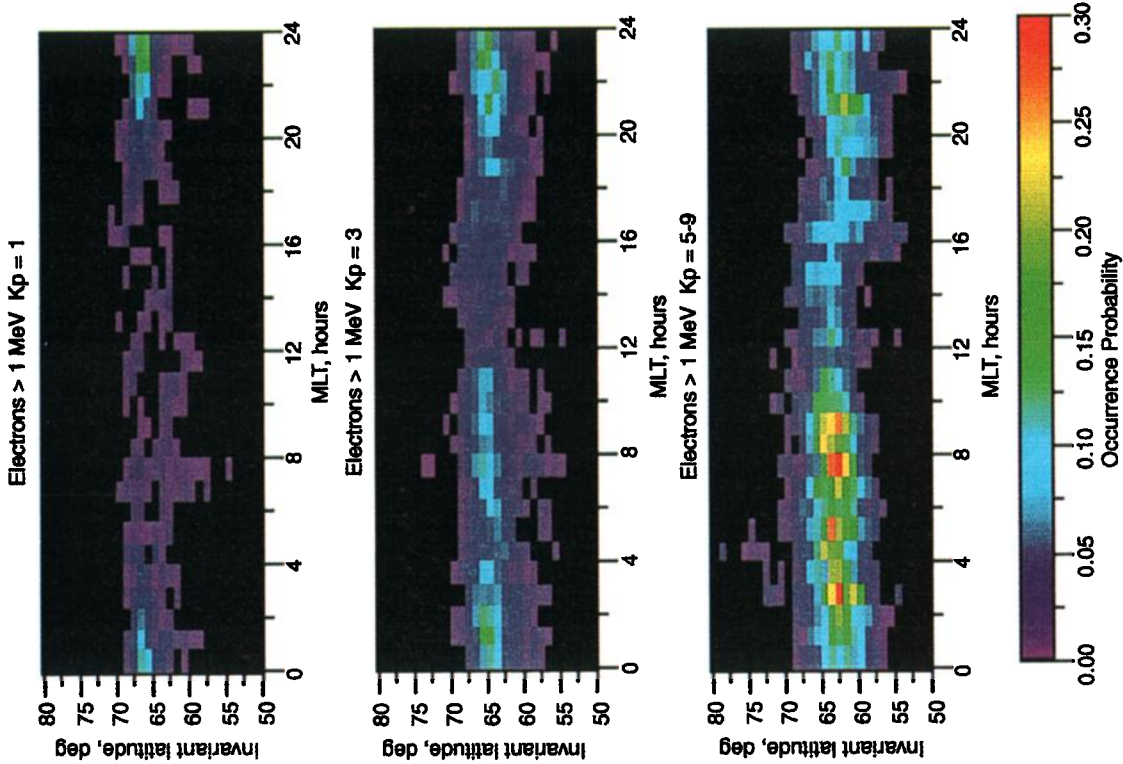
Plate 1. Occurrence probabilities for relativistic electron microbursts from day 1 to 351, 1993. The three panels show various levels of magnetic activity. The Solar, Anomalous and Magnetospheric Particle Explorer (SAMPEX) data were analyzed using a fast Fourier transform, and events with power above a particular threshold between 0 and 5 Hz were selected.
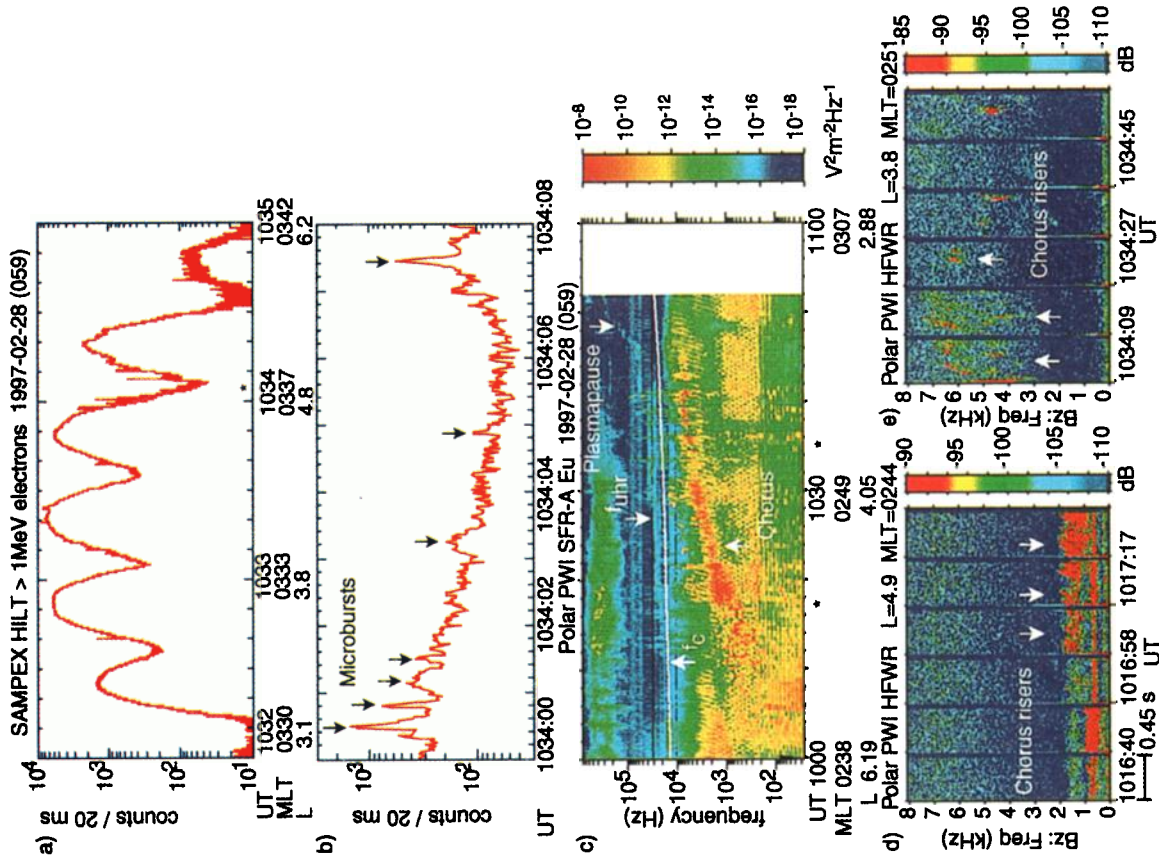

Plate 2. Predawn relativistic electron microbursts and chorus, February 28, 1997 (day 59). (a) SAMPEX >1 MeV electron data during a pass through the radiation belts. (b) SAMPEX >1 MeV electron data expanded to show microbursts. (c) Polar swept frequency receiver (SFR) data showing chorus over a range of L shells. (d) Polar high-frequency waveform receiver (HFWR) data showing individual chorus risers at the same L shell as that in the expanded microburst plot, and (e) Polar high-frequency waveform receiver HFWR data showing individual chorus risers at the same time as that in the expanded microburst plot. Stars indicate the times for which expanded plots are shown.
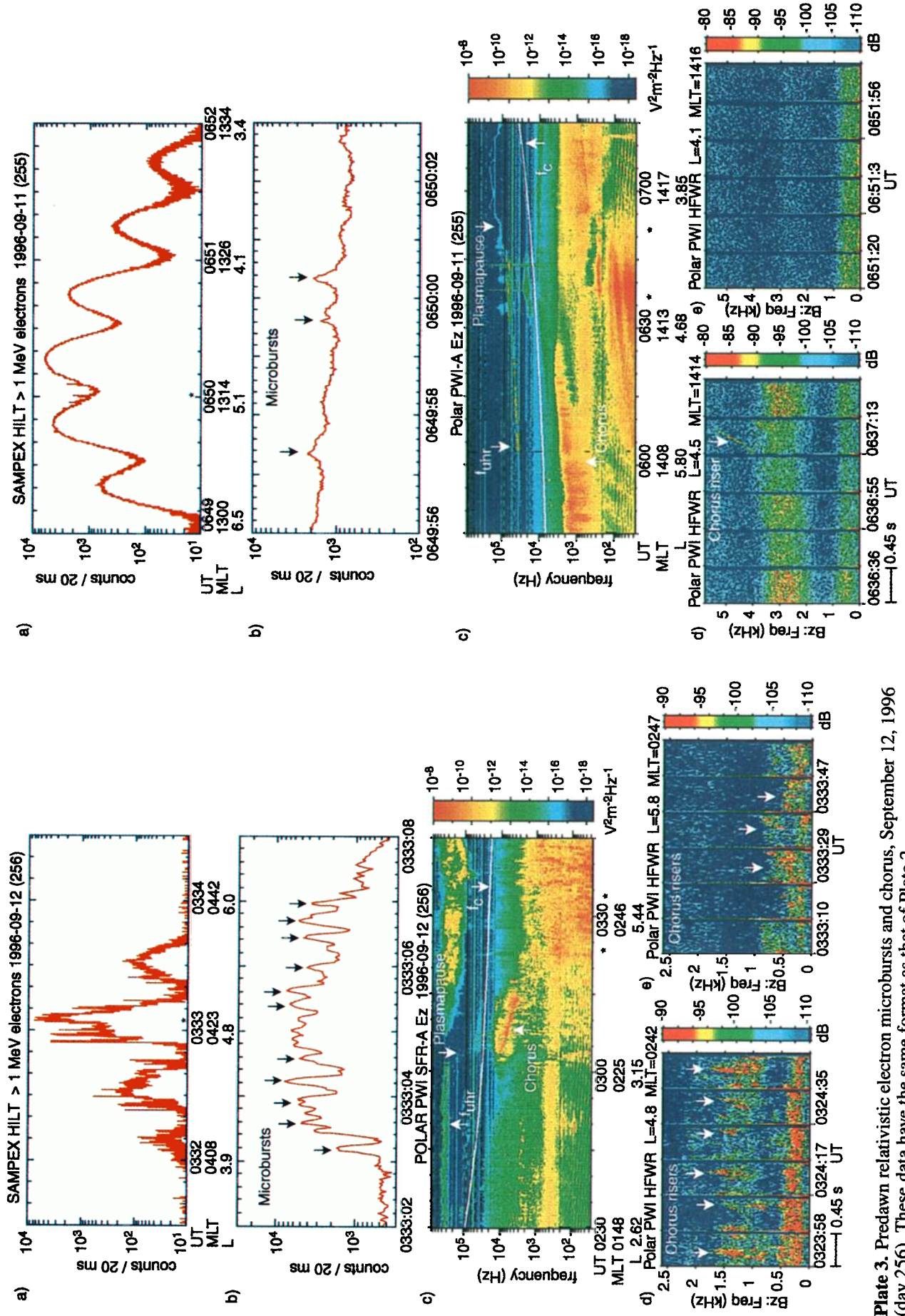
Plate 3. Predawn relativistic electron microbursts and chorus, September 12, 1996 (day 256). These data have the same format as that of Plate 2.
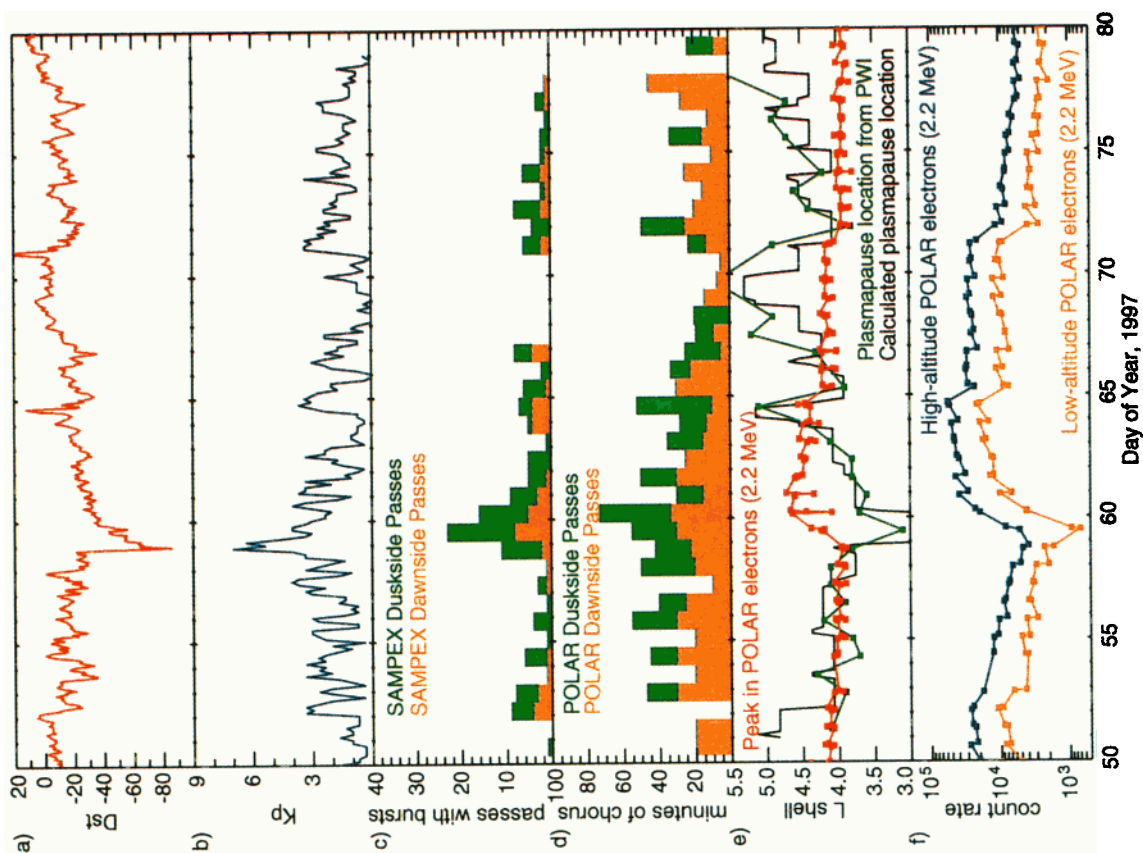

Plate 4. Postnoon relativistic electron microbursts and chorus, September 11, 1996 (day 255). These data have the same format as that of Plate 2.

Plate 6. Occurrence probabilities for microbursts and chorus during the period from February 19 to March 20, 1997 (days 50–79), in the same format as that of Plate 5.

Plate 5. Magnetospheric activity during the period from August 31 to September 30, 1996 (days 244–273). (a) *Dst*, (b) K_p, (c) occurrence probabilities for SAMPEX relativistic electron microburst observations, (d) occurrence probabilities for Polar chorus observations, (e) position of the 2 MeV electron peak measured by Polar and plasmapause locations calculated from K_p and determined from plasma wave instrument (PWI) observations of the upper hybrid resonance frequency, and (f) count rate of 2 MeV electrons observed by Polar on high- and low-altitude passes.
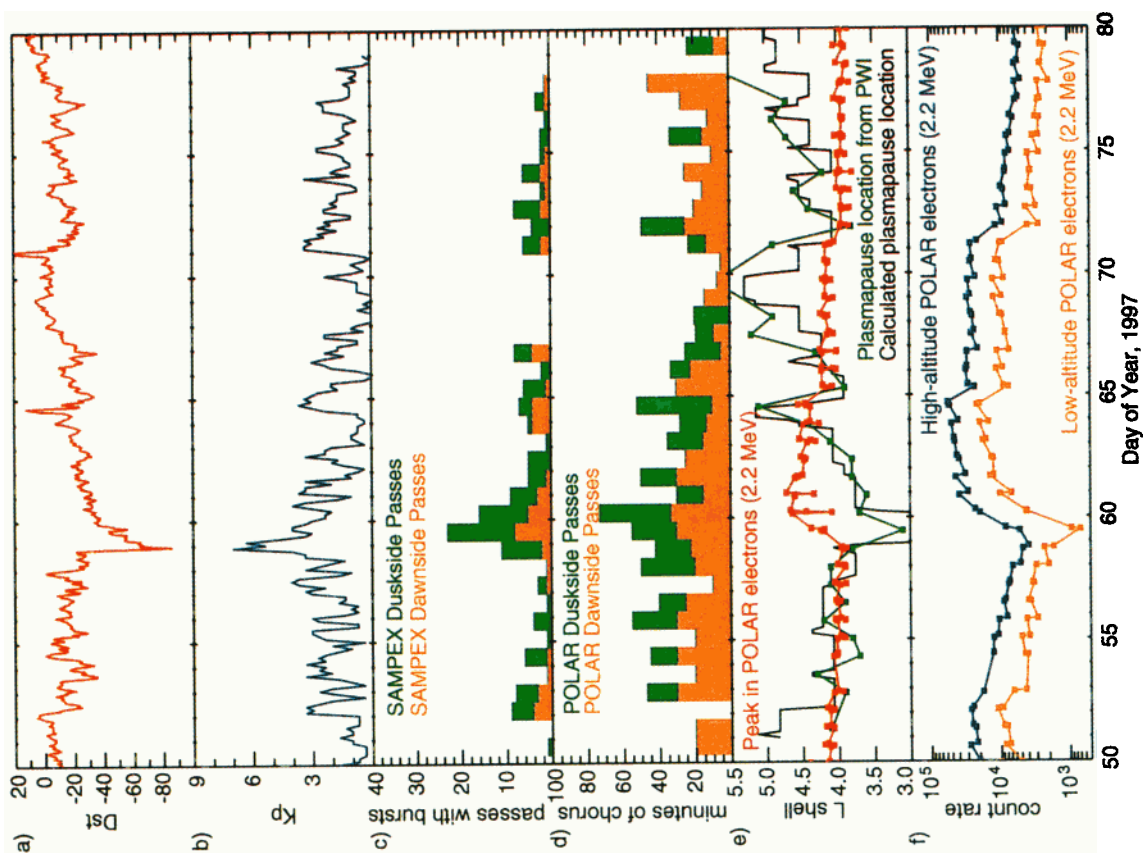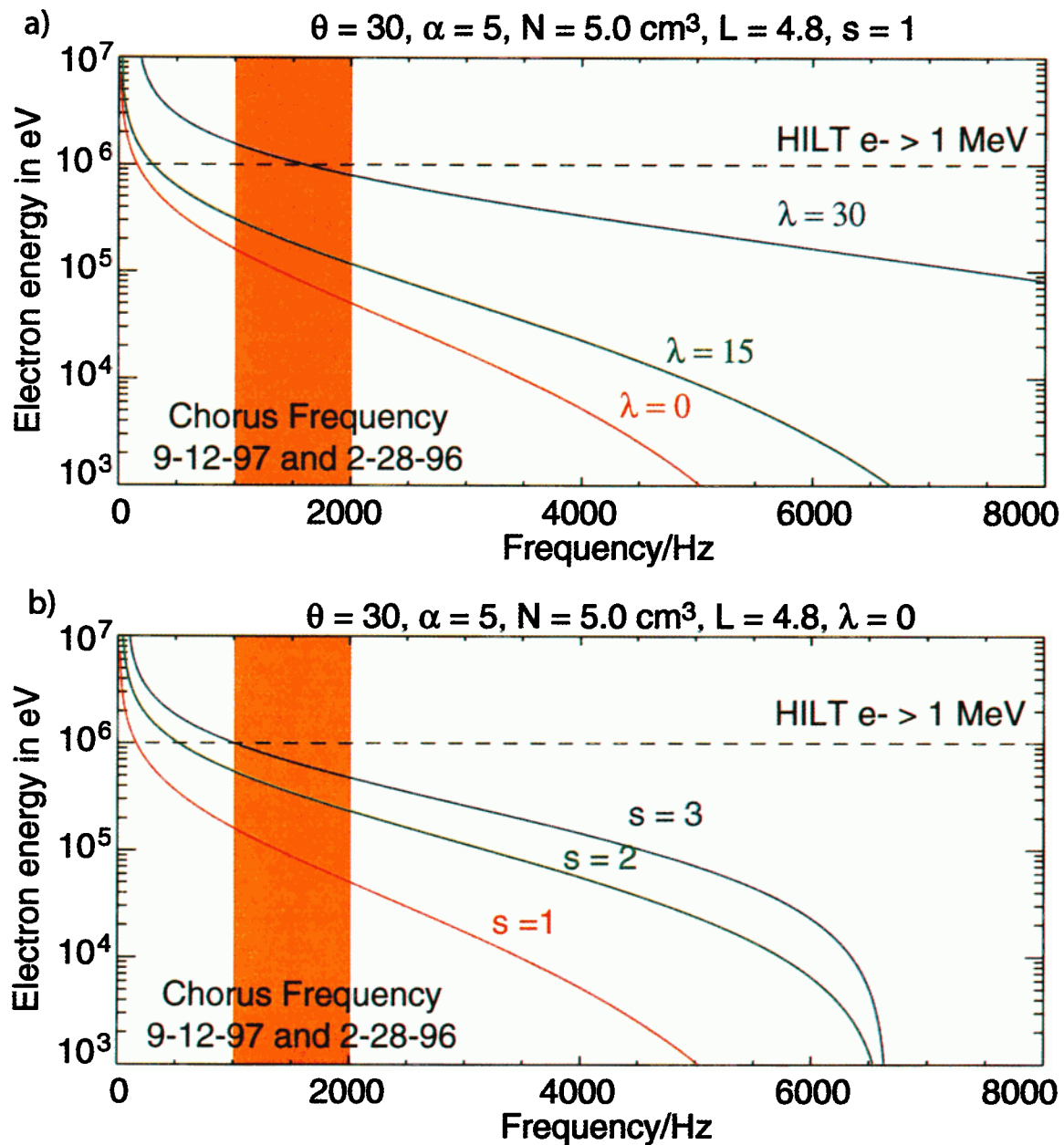
a) $\theta = 30$, $\alpha = 5$, $N = 5.0$ cm^3, $L = 4.8$, $s = 1$

b) $\theta = 30$, $\alpha = 5$, $N = 5.0$ cm^3, $L = 4.8$, $\lambda = 0$

Plate 7. Electron resonant energy versus whistler wave frequency for the conditions observed by Polar and SAMPEX in Plates 2 and 3 for (a) various locations along the field line and (b) various harmonics.

$$n^2 = \frac{c^2 k^2}{\omega^2} \simeq 1 + \frac{\omega_{pe}^2}{\omega(\Omega_e \cos\theta - \omega)}, \qquad (2)$$

where n is the index of refraction, c is the speed of light, and ω_{pe} is the electron plasma frequency [Stix, 1992].

Combining (1) and (2) gives:

$$v_{\parallel} \simeq \{-\omega k \cos\theta + [\omega^2 k^2 \cos^2\theta + $$
$$(s^2 \Omega_e^2 - \omega^2)(k^2 \cos^2\theta + s^2 \Omega_e^2/c^2 \cos^2\alpha)]^{(1/2)}\}$$
$$\cdot (k^2 \cos^2\theta + s^2 \Omega_e^2/c^2 \cos^2\alpha)^{-1}. \qquad (3)$$

Plate 7a shows the resonant electron energy as a function of frequency for three different magnetic latitudes, λ. The L value and density were those observed by Polar on the same field line as that for the predawn relativistic electron microburst examples from Plates 2 and 3. The shaded region shows the range of chorus frequencies observed at this time. The lowest curve shows that on the equator, MeV electrons will only resonate with waves of frequency <200 Hz. In order for MeV electrons to interact with waves at the observed frequencies of 1–2 kHz, the interaction must take place off the equator at magnetic latitudes near 30°. At this location the loss cone is $\sim7°$ (compared with 4° at the equator). Plate 7b shows the resonant electron energy as a function of frequency for three different values of s at the same location. On the equator, MeV electrons will only interact with the observed wave frequencies for harmonic numbers >3. Higher harmonics typically become important for obliquely propagating waves. For these calculations, $\alpha = 5°$ and $\theta = 30°$ were used. The resonant energy was found to vary insignificantly for values of $\alpha < 10°$ and $\theta < 30°$, as shown for lower-energy electrons by Chang and Inan [1983] and Inan et al. [1992].

Similar calculations were performed for bursts occurring in the postnoon sector, where observed densities are typically 10–50 cm^{-3}. At these densities the electron resonant energy is much lower than 1 MeV. However, a combination of higher harmonics and off-equatorial interactions may account for the observations. These factors may explain why fewer events were observed in this local time sector and why they tended to consist of fewer individual microbursts. An alternate possibility is that the bursts occurred in a region of depleted density. Since the dayside bursts tend to occur over a smaller range of L shells than the predawn bursts do, this assumption is not unreasonable.

5. Discussion

In summary, we believe relativistic electron microbursts are related to VLF chorus waves for four reasons: (1) Both VLF chorus and relativistic electron microbursts occur preferentially in the morning sector, at L shells outside the plasmapause. (2) When high time resolution waveform data are available, the chorus risers last for the same length of time as the coincident relativistic electron microbursts. (3) Low time resolution SFR data show a correlation between chorus occurrence and relativistic electron microbursts.

(4) Resonant energy calculations show that the observed waves can interact with MeV electrons, for given cold plasma densities and magnetic field strengths.

Although correlation does not necessarily imply causality, the observations suggest the need for a closer look at pitch angle scattering due to interaction with oblique, coherent chorus risers. A model in which electrons of different energies resonate with short-duration chorus risers at different points along the field line would explain a number of observations. The filled and partially filled loss cones observed during the relativistic electron microbursts suggest that a mechanism is strongly scattering the electrons into the loss cone but that the scattering mechanism operates on a timescale that is short with respect to the bounce period (~0.5 s for 1 MeV electrons at $L = 5$). Models have shown that coherent wave packets can produce scattering larger than those produced by incoherent waves, but typically over shorter timescales [Inan, 1987]. Cyclotron resonance with obliquely propagating coherent chorus risers would provide such a mechanism, although further modeling is necessary to accurately determine the magnitude and duration of the pitch angle scattering.

In addition, this model supports the observation that microbursts in the >150 keV channel occur at the same time as microbursts in the >1 MeV channel do, but without one-to-one correlation [Blake et al., 1996]. Chorus risers are observed to exist over a range of L shells and to propagate in an unducted mode. Thus equatorial chorus will not have the same source as chorus observed at higher magnetic latitudes along the same field line. However, scattering at different points along the field line by obliquely propagating waves would explain why the microbursts of different energies are observed at the same time, but without correlation between individual bursts. The fact that microbursts in the >150 keV channel have much larger fluxes than those in the >1 MeV channel [Blake et al., 1996] indicates that the scattering mechanism may be less efficient at higher energies.

This model also provides a reason why fewer relativistic electron microbursts are seen in the postnoon sector, despite the presence of chorus in this region. Chorus occurrence exhibits a spiral pattern in L shell [Burtis and Helliwell, 1976]. Maximum chorus is observed from about $L = 3$ to $L = 6$ in the predawn region and from $L = 5$ to $L = 9$ in the postnoon region. Since relativistic electrons are primarily contained in the radiation belts at L shells below ~6, they are less likely to encounter chorus in the postnoon region. The occurrence of microbursts is highly dependent on the relativistic electron flux trapped in the radiation belts. The source of these relativistic electrons in the radiation belts is not known but has been shown to be dependent on magnetic storm activity [Selesnick and Blake, 2000].

Our observations show that some relativistic electron microbursts occurred in the absence of chorus mode waves. These events all occurred within 3 hours of local midnight, and most consisted of only a few microbursts. These events may be more similar to the microbursts observed by Imhof et al. [1992] and the bands observed by Blake et al. [1996],

which were attributed to a loss of adiabaticity due to irregularities in the magnetic field lines. Other possible explanations for the relativistic electron microburst precipitation include wave modes such as the electromagnetic ion cyclotron (EMIC) mode [*Thorne and Andreoli*, 1980; *Imhof et al.*, 1986; *Horne and Thorne*, 1998; *Lorentzen et al.*, 2000] and the electrostatic ion cyclotron (EIC) mode [*Thorne and Andreoli*, 1980]. However, these waves do not generally have a temporal structure that would be expected to produce the strong scattering over a short timescale needed to create relativistic electron microbursts. Chorus has also been associated with wideband electrostatic [*Reinleitner et al.*, 1983] and electromagnetic [*Sonwalker et al.*, 1990] bursts of duration 100 ms to 1 s. However, only a few examples of this type of wave were observed in association with the chorus and microburst events studied here. It is unlikely that these waves are involved with the trains of multiple microbursts seen by SAMPEX.

These observations of relativistic electron microbursts and VLF chorus suggest the need for further correlated observations of waves and particles. In particular, high-energy electron detectors need large geometry factors to allow detection of the relativistic electron microbursts, and these observations must be supplemented by observations of lower-energy electrons, in order to determine the energy spectra involved and to study the connection between low- and high-energy electron microbursts. Wave observations should be extended to provide high time resolution multicomponent data at frequencies below a few kilohertz. Such observations would allow us to more carefully examine the relationship between VLF chorus and relativistic electron microbursts.

References

Anderson, K. A., and D. W. Milton, Balloon observations of X rays in the auroral zone, *J. Geophys. Res.*, *69*, 4457, 1964.

Baker, D. N., G. M. Mason, O. Figueroa, G. Colon, J. G. Watzin, and R. M. Aleman, An overview of the solar, anomalous and magnetospheric particle explorer (SAMPEX) mission, *IEEE Trans. Geosci. and Remote Sens.*, *31*, 531, 1993.

Blake, J. B., et al., CEPPAD Comprehensive energetic particle and pitch angle distribution experiment on Polar, *Space Sci. Rev.*, *71*, 531, 1995.

Blake, J. B., M. D. Looper, D. N. Baker, R. Nakamura, B. Klecker, and D. Hovestadt, New high temporal and spatial resolution measurements by SAMPEX of the precipitation of relativistic electrons, *Adv. Space Res.*, *18 (8)*, 171, 1996.

Blake, J. B., R. S. Selesnick, D. N. Baker, and S. G. Kanekal, Studies of relativistic electron injection events in 1997 and 1998, *J. Geophys. Res.*, in press, 2001.

Brown, J. C., and E. C. Stone, High-energy electron spikes at high latitudes, *J. Geophys. Res.*, *77*, 3384, 1972.

Burtis, W. J., and R. A. Helliwell, Magnetospheric chorus: Occurrence patterns and normalized frequency, *Planet. Space Sci.*, *24*, 1007, 1976.

Carpenter, D. L., and R. R. Anderson, An ISEE/whistler model of equatorial electron density, *J. Geophys. Res.*, *97*, 1097, 1992.

Chang, H. C., and U. S. Inan, Quasi-relativistic electron precipitation due to interactions with coherent VLF waves in the magnetosphere, *J. Geophys. Res.*, *88*, 318, 1983.

Gurnett, D. A., et al., The polar plasma wave instrument, *Space Sci. Rev.*, *71*, 597, 1995.

Harten, R., and K. Clark, The design features of the GGS Wind and Polar spacecraft, *Space Sci. Rev.*, *71*, 23, 1995.

Horne, R. B., and R. M. Thorne, Potential waves for relativistic electron scattering and stochastic acceleration during magnetic storms, *Geophys. Res. Lett.*, *25*, 3011, 1998.

Imhof, W. L., H. D. Voss, D. W. Datlowe, E. E. Gaines, J. Mobilia, and D. S. Evans, Relativistic electron and energetic ion precipitation spikes near the plasmapause, *J. Geophys. Res.*, *91*, 3077, 1986.

Imhof, W. L., H. D. Voss, J. Mobilia, D. W. Datlowe, and E. E. Gaines, The precipitation of relativistic electrons near the trapping boundary, *J. Geophys. Res.*, *96*, 5619, 1991.

Imhof, W. L., H. D. Voss, J. Mobilia, D. W. Datlowe, E. E. Gaines, J. P. McGlennon, and U. S. Inan, Relativistic electron microbursts, *J. Geophys. Res.*, *97*, 13,829, 1992.

Inan, U. S., Gyroresonant pitch angle scattering by coherent and incoherent whistler mode waves in the magnetosphere, *J. Geophys. Res.*, *92*, 127, 1987.

Inan, U. S., Y. T. Chiu, and G. T. Davidson, Whistler-mode chorus and morningside aurorae, *Geophys. Res. Lett.*, *19*, 653, 1992.

Kim, H. J., and A. A. Chan, Fully adiabatic changes in storm time relativistic electron fluxes, *J. Geophys. Res.*, *102*, 22,107, 1997.

Klecker, B., et al., HILT: A heavy ion large area proportional counter telescope for solar and anomalous cosmic rays, *IEEE Trans. Geosc. and Remote Sens.*, *31*, 542, 1993.

Koons, H. C., and J. L. Roeder, A survey of equatorial magnetospheric wave activity between 5 and 8 R_E, *Planet. Space Sci.*, *38*, 1335, 1990.

Laakso, H., et al., Electron density distribution in the magnetosphere, in *The 31st ESLAB Symposium on Correlated Phenomena at the Sun, in the Heliosphere, and in Geospace*, p. 53, Eur. Space Agency, Noordwijk, The Netherlands, 1997.

Lauben, D. S., U. S. Inan, T. F. Bell, D. L. Kirchner, G. B. Hospodarsky, and J. S. Pickett, VLF chorus emissions observed by Polar during the January 10, 1997 magnetic cloud, *Geophys. Res. Lett.*, *25*, 2995, 1998.

Li, X., et al., Multisatellite observations of the outer zone electron variation during the November 3-4, 1993, magnetic storm, *J. Geophys. Res.*, *102*, 14,123, 1997.

Lorentzen, K. R., M. P. McCarthy, G. K. Parks, J. E. Foat, R. M. Millan, D. M. Smith, R. P. Lin, and J. P. Treilhou, Precipitation of relativistic electrons by interaction with electromagnetic ion cyclotron waves, *J. Geophys. Res.*, *105*, 5381, 2000.

Lyons, L. R., H. E. J. Koskinen, J. Blake, A. Egeland, M. Hirahara, M. Øieroset, P. E. Sandholt, and K. Shiokawa, Processes leading to plasma losses into the high-latitude atmosphere, *Space Sci. Rev.*, *88*, 85, 1999.

Matthews, D. L., T. J. Rosenberg, J. R. Benbrook, and E. A. Bering III, Dayside energetic electron precipitation over the South Pole (lambda = 75 degrees), *J. Geophys. Res.*, *93*, 12,941, 1988.

Nakamura, R., D. N. Baker, J. B. Blake, S. Kanekal, B. Klecker, and D. Hovestadt, Relativistic electron precipitation enhancements near the outer edge of the radiation belt, *Geophys. Res. Lett.*, *22*, 1129, 1995.

Nakamura, R., M. Isowa, Y. Kamide, D. N. Baker, J. B. Blake, and M. Looper, SAMPEX observations of precipitation bursts in the outer radiation belt, *J. Geophys. Res.*, *105*, 15,875, 2000.

Oliven, M. N., and D. A. Gurnett, Microburst phenomena, 3, An association between microbursts and VLF chorus, *J. Geophys. Res.*, *73*, 2355, 1968.

Parks, G. K., Microburst precipitation phenomena, *J. Geomagn. Geoelectr.*, *30*, 327, 1978.

Parks, G. K., C. Gurgiolo, and R. West, Relativistic electron precipitation, *Geophys. Res. Lett.*, *6*, 393, 1979.

Reinleitner, L. A., D. A. Gurnett, and T. E. Eastman, Electrostatic bursts generated by electrons in Landau resonance with whistler mode chorus, *J. Geophys. Res.*, *88*, 3079, 1983.

Roeder, J. L., J. R. Benbrook, E. A. Bering III, and W. R. Sheldon, X ray microbursts and VLF chorus, *J. Geophys. Res.*, *90*, 10,975, 1985.

Rosenberg, T. J., L. J. Lanzerotti, D. K. Bailey, and J. D. Pierson, Energy spectra in relativistic electron precipitation events, *J. Atmos. Terr. Phys.*, *34*, 1977, 1972.

Rosenberg, T. J., J. C. Siren, D. L. Matthews, K. Marthinsen, J. A. Holtet, A. Egeland, D. L. Carpenter, and R. A. Helliwell, Conjugacy of electron microbursts and VLF chorus, *J. Geophys. Res.*, *86*, 5819, 1981.

Rosenberg, T. J., R. Wei, D. L. Detrick, and U. S. Inan, Observations and modeling of wave-induced microburst electron precipitation, *J. Geophys. Res.*, *95*, 6467, 1990.

Selesnick, R. S., and J. B. Blake, On the source location of radiation belt relativistic electrons, *J. Geophys. Res.*, *105*, 2607, 2000.

Sergeev, V. A., E. M. Sazhina, N. A. Tsyganenko, J. Å. Lund-blad, and F. Søraas, Pitch-angle scattering of energetic protons in the magnetotail current sheet as the dominant source of their isotropic precipitation into the nightside ionosphere, *Planet. Space Sci.*, *31*, 1147, 1983.

Sonwalker, V. S., R. A. Helliwell, and U. S. Inan, Wideband VLF electromagnetic bursts observed on the DE 1 satellite, *Geophys. Res. Lett.*, *17*, 1861, 1990.

Stix, T. H., *Waves in Plasmas*, p. 40, Am. Inst. of Phys., College Park, Md., 1992.

Thorne, R. M., and L. J. Andreoli, Mechanisms for intense relativistic electron precipitation, in *Exploration of the Polar Upper Atmosphere*, edited by C. S. Deehr and J. A. Holtet, p. 381, D. Reidel, Norwell, Mass., 1980.

Torkar, K. M., et al., A study of the interaction of VLF waves with equatorial electrons and its relationship to auroral X-rays in the morning sector, *Planet. Space Sci.*, *35*, 1231, 1987.

J. B. Blake and K. R. Lorentzen, The Aerospace Corporation, P. O. Box 92957, Los Angeles, CA 90009-2957, (kirsten.r.lorentzen@aero.org)

J. Bortnik and U. S. Inan, STAR Lab, Stanford University, Stanford, CA 94305-9515.